JOURNAL OF APPLIED ELECTROCHEMISTRY 26 (1996) 711–720

Electrodeposition of membrane-oriented conducting poly(pyrrole, thiophene) on stainless steel meshes

M. ZHOU, M. PERSIN, J. SARRAZIN*

Laboratoire des Matériaux et Procédés Membranaires, UMR 9987 UM II, ENSCM, CNRS, France, and Ecole Nationale Supérieure de Chimie, 8 rue de l'Ecole Normale, 34053 Montpellier Cedex 1, France

Received 13 June 1995; revised 12 February 1996

Dense membrane preparation was attempted by electrochemical deposition of polypyrrole and polythiophene on stainless steel meshes. The effect of modifying experimental factors such as supporting electrolyte, electrochemical parameters and water addition were investigated. Compact polypyrrole deposits spreading over the meshes could be obtained, but preparative deposition of polythiophene on the same substrate was hindered by competitive anodic corrosion.

1. Introduction

Until recently, applications of conducting polymers (CPs) were mainly related to their conductivity [1–5], and there were few considerations of their chemical affinity and structural properties. Membrane-oriented applications represent a new area where the latter aspects play important roles.

Burgmayer and Murray [6, 7] measured the permeation of Cl^- and KCl through oxidized and reduced pyrrole electrochemically deposited on gold minigrids. Their results showed that the ionic permeability could be switched by controlling the polypyrrole oxidation state (polycationic, neutral and any state in between) by means of a potential applied to the membrane [8–10]. Recently the electrochemically controlled transport of ions through conducting polypyrrole membranes has also been studied. In addition to these studies based on ion transport, applications in gas separation using polyaniline and poly(*N*-methylpyrrole) as separation barriers have been proposed [11–14]. Investigations have also been carried out on the permeation of neutral liquid through CP membranes [14–16].

Despite the work mentioned above, membrane-related applications have not been well exploited. One of the reasons is that with some exceptions, CPs are normally insoluble in many solvents and this makes it impossible to prepare membranes through conventional techniques based on solution vaporization. As membrane material, a polymer can be either processed or directly synthesized in the required final shape. Due to the insolubility and poor processibility, the strategy for preparation of CP membranes is a one-step fabrication, in which polymerization and formation occur simultaneously. Thus CP membranes designed for research purposes have been prepared and investigated by several authors. The membrane forms and synthesis procedures are summarized below.

Electrodeposited free-standing membranes: Polypyrrole doped with *p*-toluene sulphonate (PPy–PTS) is relatively flexible and, after electrochemical polymerization in aqueous solution, it can be peeled off by soaking in water if the working electrode is smooth [8–10]. However, from a practical point of view, free-standing membranes are not easy to manipulate [13] and membranes of large area are difficult to obtain. This is particularly true for the less flexible materials.

Electrodeposited composite membranes: Electropolymerization on porous anodes, can lead to composite membranes: the polymer can act as a separation layer while the porous substrate serves as a mechanical support. The latter adds almost no additional resistance to permeation through the membrane. To be functional as a working electrode, the permeable porous substrate must be conductive; if not, a conductive coating should be previously applied to the surface on which the polymer film will be generated. The substrates used so far are gold minigrids [7], gold-coated polycarbonate microfilters [7], gold-coated Anopore membranes [17, 18], gold-coated PTFE membranes [16] etc. This work is based on noble metals and is not of practical interest.

Chemically synthesized composite membranes: Due to the lack of suitable porous materials for working electrodes in electrosynthesis, chemical synthesis of CP onto various permeable supports was adopted. With the exception of polyaniline membranes, which can result from solution casting from its emeraldine base solution prepared by chemical reactions [11, 19], the CP composite membranes investigated so far were obtained through the direct contact of monomer and oxidant in the pores or at the interface between reagent and substrate (interfacial polymerization). Both the polymerization and oxidative doping processes were accomplished during contact oxidation. The details vary in different cases. Polypyrrole, poly(*N*-methylpyrrole), poly(3-methylthiophene) have been synthesized onto some commercially available porous membranes, such as microporous polypropylene [19],

* To whom correspondence should be addressed.

0021-891X

Teflon [19], polycarbonate [15], γ-alumina [13, 14, 18], using KI_3, $Fe(ClO_4)_3$, $Fe(NO_3)_3$ and $FeCl_3$ as oxidizing agents. Usually in these chemically synthesized CPs, the incorporated counterions are restricted to the anions of the oxidants used in the polymerization.

In comparison with chemical synthesis and in addition to the wider choice of incorporated anions, the electrochemical deposition of CP membranes offers an easier control of process conditions and film thickness, and a better reproducibility of deposit quality. *In situ* characterization of the depositing process is also possible with the aid of electrochemical signals and spectroscopic techniques [20–22]. The present work focused on commercially available stainless steel meshes. Due to their acceptable mechanical strength, permeability and conductivity, these are good candidates for preparing CP/substrate composite membranes through electrochemical synthesis. Furthermore such flexible metallic membranes offer the possibility of continuous synthesis on a large scale for future commercial purposes. The deposition of polypyrrole and polythiophene on nonnoble electrodes such as titanium [23, 24], soft iron [23, 25–30], stainless steel [8] and aluminium [23, 31] have been reported. In recent work [32], it was observed that dense polypyrrole films electrodeposited on stainless steel meshes displayed high selectivity to ethanol in the pervaporation of ethanol/cyclohexane mixtures. This prompted further study of the preparation and application in pervaporation of a wide range of CPs. Focusing on dense membranes with good morphology for pervaporation, the present paper reports the electrochemical and morphological investigation of polypyrrole (PPy) and polythiophene (PTh) on stainless steel meshes. The polymerization scheme for these two monomers can be represented as follows:

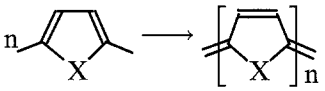

2. Experimental details

For cyclic voltammetry, electropolymerization was performed, (unless otherwise noted), in a four-necked minicell (volume 10 ml) with three-electrode compartments separated by sintered glass. Strips of stainless steel mesh (diameter of mesh wires 25 × 18 μm, nominal opening 6.3 μm, porosity 36%) with an apparent deposition area of 0.25 cm^2 were used as working electrodes without any pretreatment. Platinum gauze and Ag^+ (0.1 M $AgNO_3$ in CH_3CN)/Ag were used as the auxiliary and reference electrodes, respectively. Typical solutions were 0.1 M monomer in the presence of 0.05 M Me_4NBF_4 and 0.1 M Bu_4NBF_4 or 0.1 M Bu_4NPF_6 in acetonitrile.

Acetonitrile (sds, purex. >99.5%, water content $\leq$0.05%), thiophene (Fluka, purum, >98%), pyrrole (Fluka, purum >96%), Me_4NBF_4 (Fluka, purum), Bu_4NBF_4 (Fluka, purum. p.a.) and Bu_4NPF_6 (Fluka, puriss. p.a.) were used without further purification.

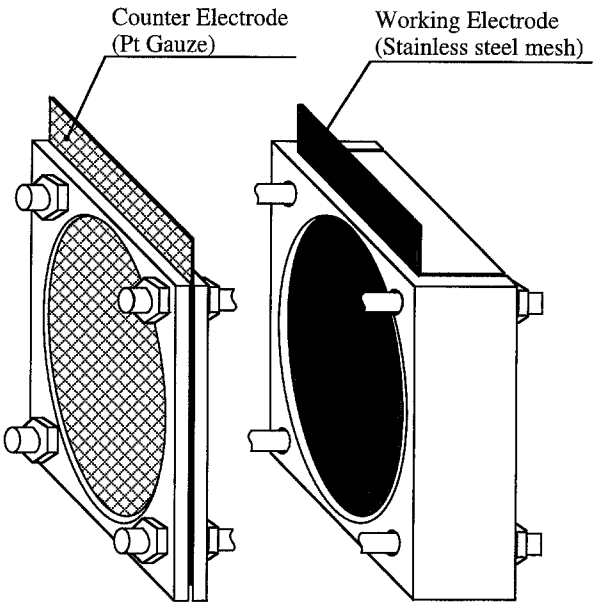

Fig. 1. Electrode holder for the preparation of composite membranes by electropolymerization.

Preparative electrosyntheses of composite membranes designed for the pervaporation test were carried out at constant potential in a beaker cell containing a suitable solution. A metallic disc of diameter 52 mm was mounted in a specially designed anode holder (Fig. 1) to keep the working electrode and counter electrode (platinum gauze) parallel. All experiments were carried out in air at room temperature.

The apparatus for electrochemical control and measurement were an EG&G PAR (model 362) scanning potentiostat and a Kipp & Zonen X–Y recorder with a time-Y recording capability. Two modes were applied, namely, cyclic voltammetry and potentiostatic techniques, for the electrochemical studies and membrane preparation, respectively.

Deposits were rinsed thoroughly with the acetonitrile solvent to remove electrolyte residues. For SEM observation, samples were dried by direct exposure to air. The instrument used was a Leica Stereoscan 260. Fractography was obtained by fracturing only the polymer layer in liquid nitrogen.

3. Results and discussion

In electrochemical synthesis, the electrochemical behaviour of reactants generally differs depending on factors such as solvent, supporting electrolyte, nature of the electrode etc. In the present work, cyclic voltammetry was used in a preliminary investigation to elucidate the observed phenomena and determine conditions for the membrane synthesis. It should be noted that the currents, and not the current densities in the cyclic voltammograms (CVs), are indicated in this paper, due to the complex structure of the working electrode.

3.1. Polypyrrole (PPy)

3.1.1. Cyclic voltammetry. To obtain a morphologically sound membrane, the formation of PPy was studied

using all three kinds of supporting electrolytes mentioned in the experimental section. Figure 2 is restricted to CVs obtained with Bu_4NBF_4 and Bu_4NPF_6 in the presence and absence of water.

It was found that all the potential scans led to the formation of the polymer. The common features extracted from Fig. 2 are the 'nucleation loops' [33] and almost the same oxidation potential as the pyrrole monomer (~0.8 V). Great differences exist in the shape of these CVs, suggesting the influence of the electrolyte solutions on the polymerization/deposition process. The morphologies of the films deposited on0.25 cm^2 mesh at constant potential (1.0 V) for 5 min have quite different features, as illustrated in Fig. 3.

Among the three supporting electrolytes, Bu_4NPF_6 led to the most compact deposition both in water-free and water-containing solutions, while Bu_4NBF_4 resulted in a loosely agglomerated, porous deposit, unsuitable for membrane construction. In all cases, the addition of water gave rise to greater deposition, accompanied by improved film quality (see Fig. 3(a) and (b); Fig. 3(e) and (f)).

3.1.2. Membrane synthesis. Based on the above morphologic observation, preparative synthesis was performed potentiostatically using Bu_4NPF_6 as supporting electrolyte in a beaker cell. Under these circumstances, a good composite membrane designed for use in pervaporation was obtained.

SEM observation of PPy membranes revealed that the holes in the substrate were filled, the surface being well covered by a dense deposit. Figure 4 shows the film cross-section, back side and front side depositions. The film surface, though not completely flat, was relatively smooth as compared with the substrate. It is well known, as established for the electrodeposition of polypyrrole [34], polythiophene [35] and poly (3-methylthiophene) [36], that the deposit thickness on flat surfaces increases linearly with the electrical charge passed. However, such a linear relationship could not be observed when meshes were used as

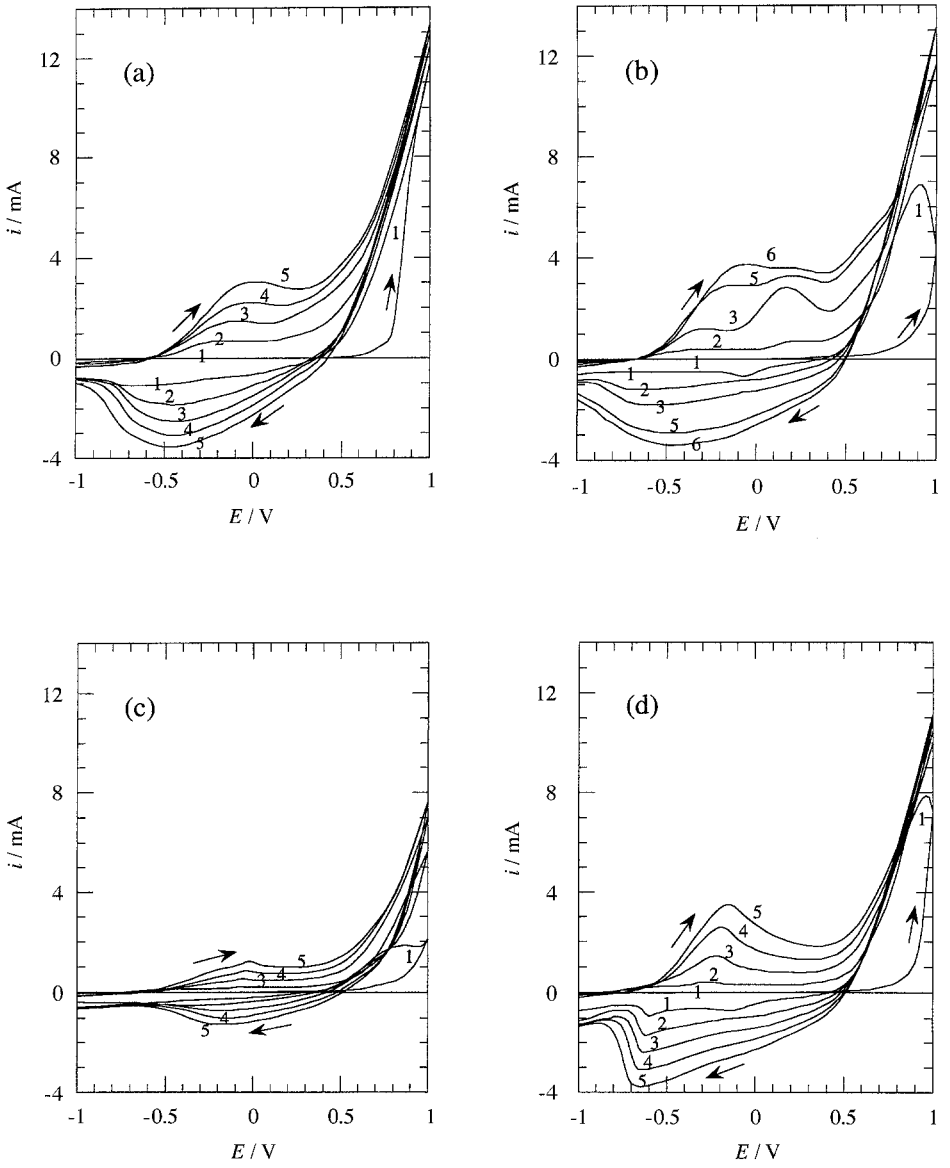

Fig. 2. Cyclic voltammograms for polypyrrole formed in different acetonitrile solutions (Monomer concentration: 0.1 M, anode apparent area: 0.25 cm^2, scan rate: 100 $mV s^{-1}$). (a) 0.1 M Bu_4NBF_4; (b) 0.1 M Bu_4NBF_4 in the presence of 1 wt % H_2O; (c) 0.1 M Bu_4NPF_6; (d) 0.1 M Bu_4NPF_6 in the presence of 1 wt % H_2O.

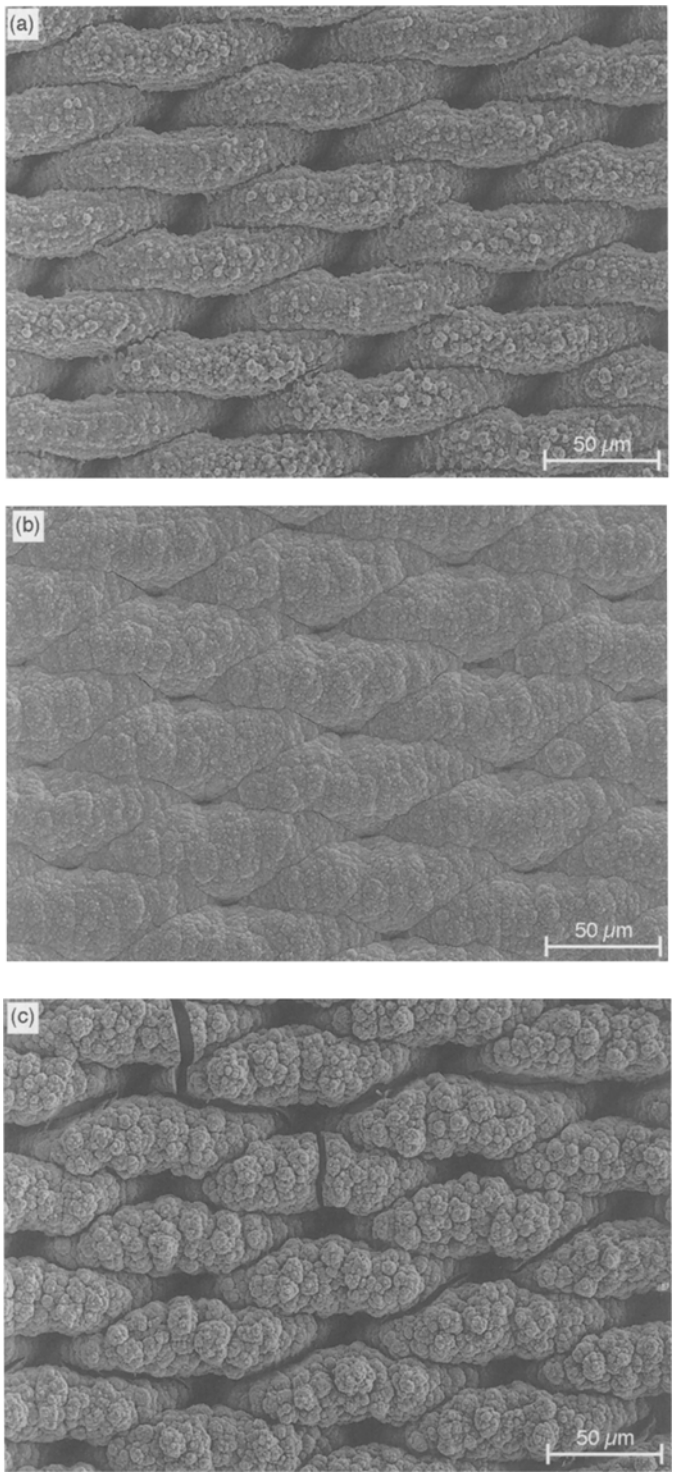

electrodes, since the deposit occurred both along and around the metallic wires before the holes were completely filled and the back side deposition stopped. As single side deposition was required, the electrode holder (Fig. 1) was made in such a way that the mesh was maintained against the Teflon back brick. The mesh side facing the platinum counter electrode could be covered, and only a small deposit occurred on the back side due to the permeable structure of the initial working electrode. However, growth also spread to the edge of the Teflon surface around the electrode.

Different behaviours were observed depending on the presence or absence of water in the electrolytic solutions. First, in the absence of water, deposition on the working electrode was accompanied by the generation of an insoluble brown substance, possibly oligomers precipitating in the cell; second, different current-time responses were found (Fig. 5) when electrosynthesis was performed in water-free and water-containing solutions. Such a behaviour was not observed in the case of the minicell. Finally, in water-free solutions, after the deposit had reached a certain thickness, a porous material, with a loose texture began to form. Once formed, this material developed quickly, leading to a large increase in electrode area and, consequently, to a sharp increase in the current (Fig. 5(a)).

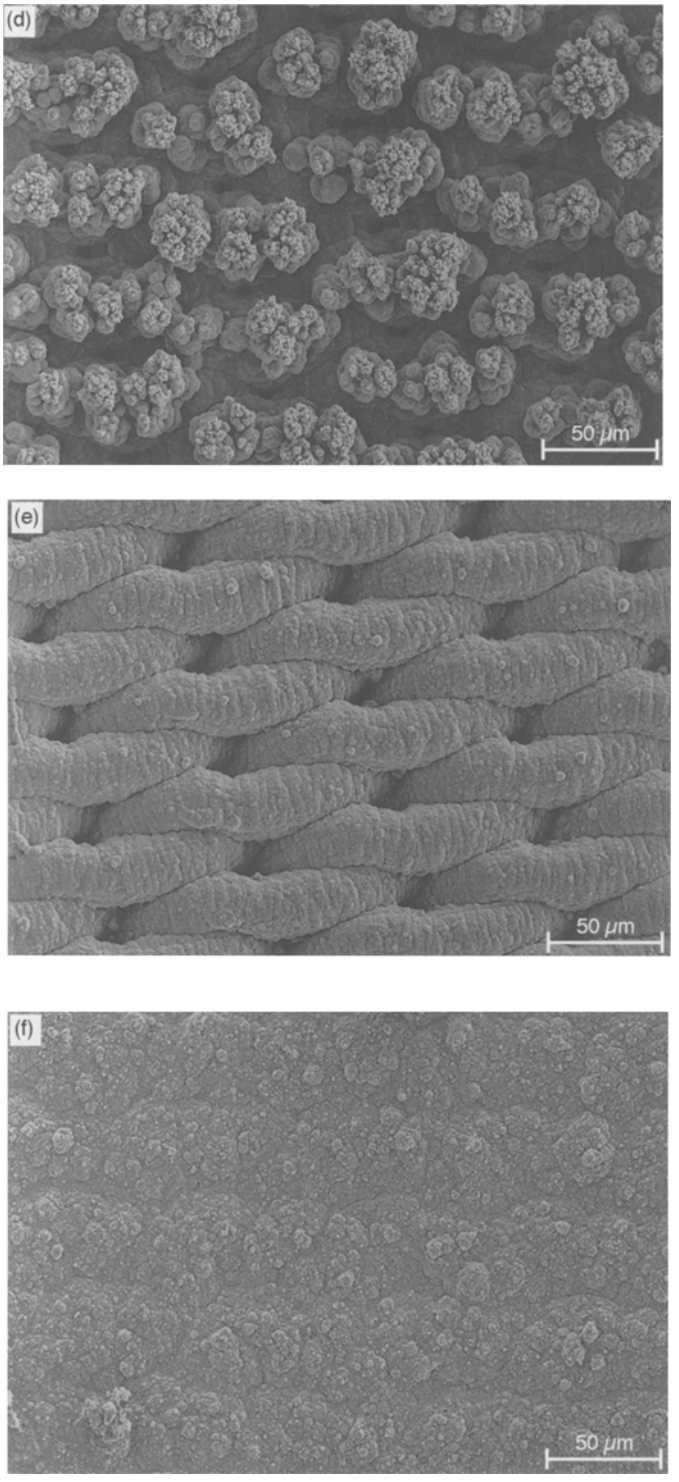

Fig. 3. SEM observation of polypyrrole electrodeposited on 0.25 cm^2 mesh at constant potential (1.0 V) for 5 min. (a) 0.05 M Me_4NBF_4; (b) 0.05 M Me_4NBF_4 in the presence of 1 wt % H_2O; (c) 0.1 M Bu_4NBF_4; (d) 0.1 M Bu_4NBF_4 in the presence of 0.1 wt % H_2O; (e) 0.1 M Bu_4NPF_6; (f) 0.1 M Bu_4NPF_6 in the presence of 0.1 wt % H_2O.

According to the generally accepted mechanism, the first reaction step is the oxidation of the monomer to a radical cation. This is followed by the dimerization, trimerization and higher oligomerization of the radical cation. This commonly accepted 'radical cation–radical cation' coupling path has been questioned, the argument being that the coulombic repulsion would not allow the direct combination of two small charged radicals. The observed effect of water, however, supports the 'radical cation–radical cation' coupling hypothesis because the high permittivity ($\epsilon_{25\,°C} = 79$) of water diminishes the coulomb repulsion between the charged radicals.

3.2. *Polythiophene (PTh)*

Due to the potential required for the oxidation of thiophene, the deposition of PTh on stainless

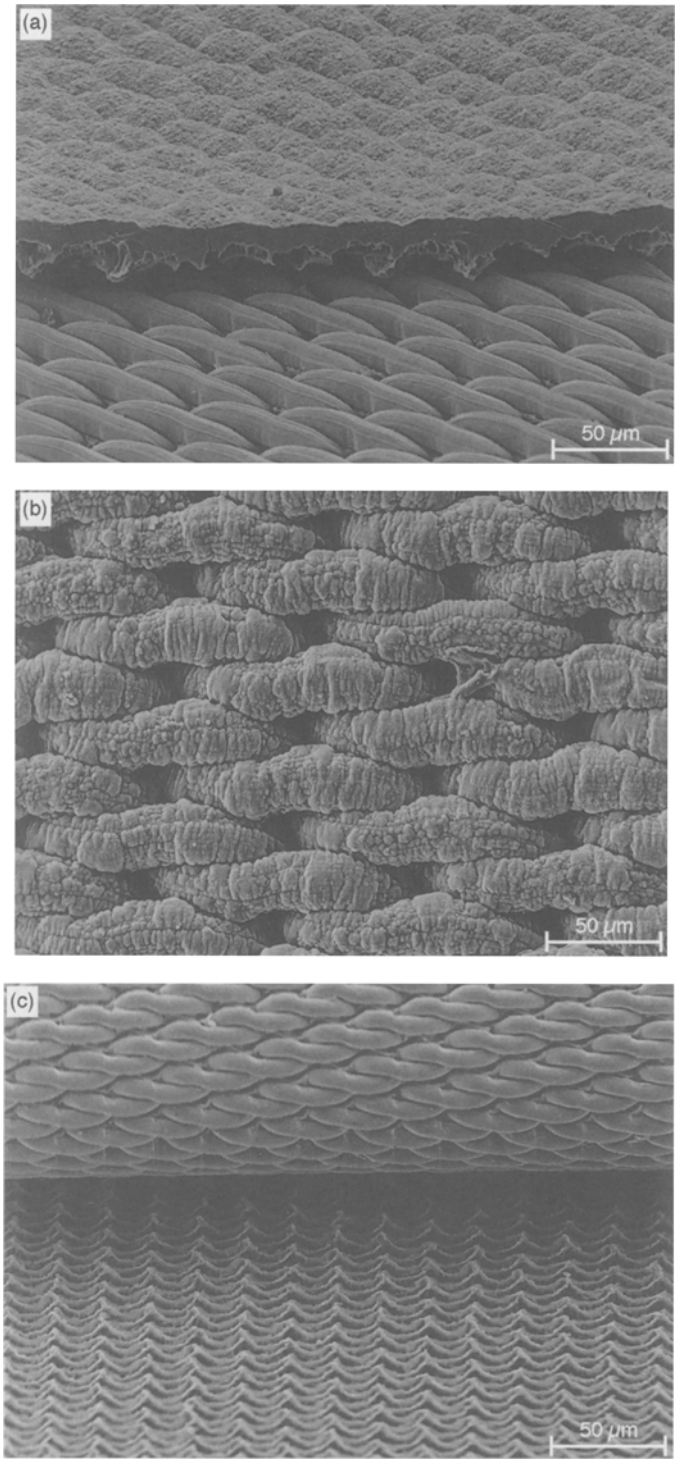

Fig. 4. SEM observation of polypyrrole–stainless steel mesh composite membrane prepared in acetonitrile solutions (1% water, monomer concentration: 0.1 M, supporting electrolyte: 0.1 M Bu_4NPF_6, duration 20 min). (a) Surface and cross-section of polypyrrole film on the mesh; (b) deposition of polypyrrole on the back side of the mesh; (c) substrate-adjacent side of the peeled-off film.

steel meshes did not proceed as easily as that of PPy.

Cyclic voltammograms of PTh on a platinum electrode, mounted in the Teflon holder, and on stainless steel meshes are shown in Fig. 6. The shapes of these two sets of curves appear similar. The oxidation of thiophene monomer begins at 1.35 V vs Ag^+ (0.1 M)/Ag on both substrates. After the first forward scan, PTh grows on the fibres and gives rise to a wide reduction peak on the first reverse scan and an oxidizing peak at a potential value lower than 1.35 V on the following forward scans. But a careful comparison of the first reverse scans shows two differences.

First, in the case of stainless steel, shoulders or anodic peaks exist on the reverse scan, as clearly shown in Fig. 7 where a low scan rate was applied. When increasing the number of scans, these peaks and shoulders gradually disappeared.

Second, the point on the reverse scans on which the current intensity was switched from positive to negative values was constant in the case of platinum (1.2 V, Fig. 6(a)); in contrast, in the case of stainless

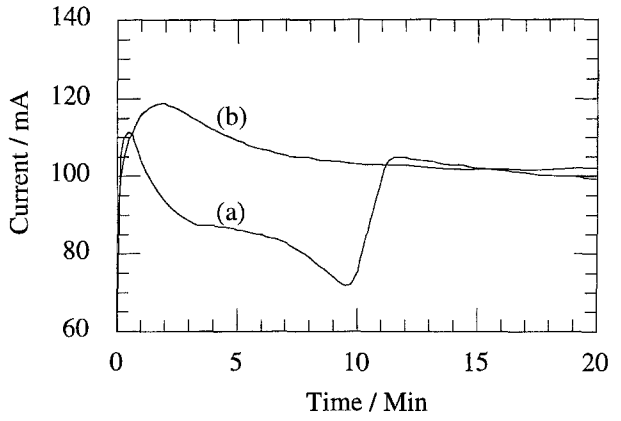

Fig. 5. Current–time response of preparative synthesis of polypyrrole on 21.2 cm^2 mesh in acetonitrile solutions (monomer concentration: 0.1 M, supporting electrolyte: 0.1 M Bu_4NPF_6). (a) In the absence of water; (b) in the presence of 1 wt % water.

steel (Fig. 6(b)), it shifted from irregular initial values to more positive potentials until it reached 1.2 V, at which all further reverse scan curves intersected the zero current line.

We attribute this phenomenon to the simultaneous oxidation of the organic substrate and of the steel electrode. In fact, some experiments were also performed in solutions without thiophene and solutions with only 0.01 M thiophene. The CV curves obtained in both these solutions are shown in Fig. 8. In thiophene-free solutions, the current can only be attributed to the anode corrosion. After a slow early phase, the oxidation of the electrode proceeds faster and even after the scan direction was reversed at 2.0 V, the anodic current continuously increased. An anomalous peak was then observed on the reverse scan, leading to a characteristic loop on the cyclic voltammogram. However, the oxidation became slower upon increasing the number of scans, probably due to a passivation of the electrode.

When solutions contained thiophene, corrosion of the electrode and deposition of PTh on the electrode occurred simultaneously. Thus the shapes of the CV curves were distorted (Fig. 6(b), Fig. 7 and Fig. 8(b))

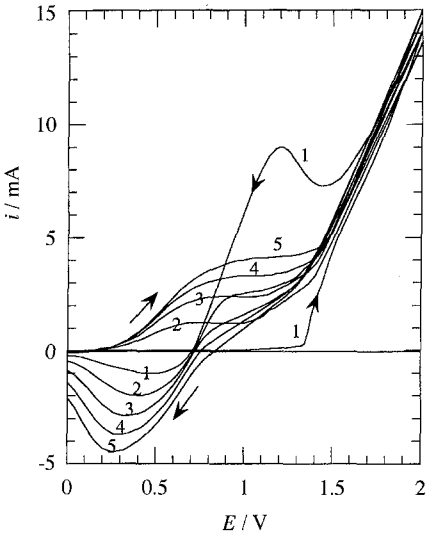

Fig. 7. Cyclic voltammograms for polythiophene formed on 0.25 cm^2 mesh in acetonitrile solution (monomer concentration: 0.1 M, supporting electrolyte: 0.05 M Me_4NBF_4, scan rate: 20 mV s^{-1}).

and depended on the ratio of electrode oxidation to polymerization and deposition. Two extreme shapes were observed corresponding to polymerization without electrode oxidation as occurs on platinum electrodes (Fig. 6(a)) and to electrode oxidation without thiophene polymerization (Fig. 8(a)). Fig. 8(b) exhibits the situation of dominant electrode oxidation: from the cathodic peak, it can be seen that only a small amount of polymer was obtained. As the monomer concentration increased, polymer deposition became more important. Whatever the monomer concentration, after several scans the electrode became gradually covered by the continuously generated deposit, and the electrode oxidation was inhibited (Fig. 8). Consequently, after a given number of scans, CVs eventually looked similar to those obtained on platinum with the necessary number of scans decreasing when the monomer concentration was increased (Fig. 6(b) and Fig. 7).

It can also be said that the shift of the switching point on the reverse scan is due to the CV distortion

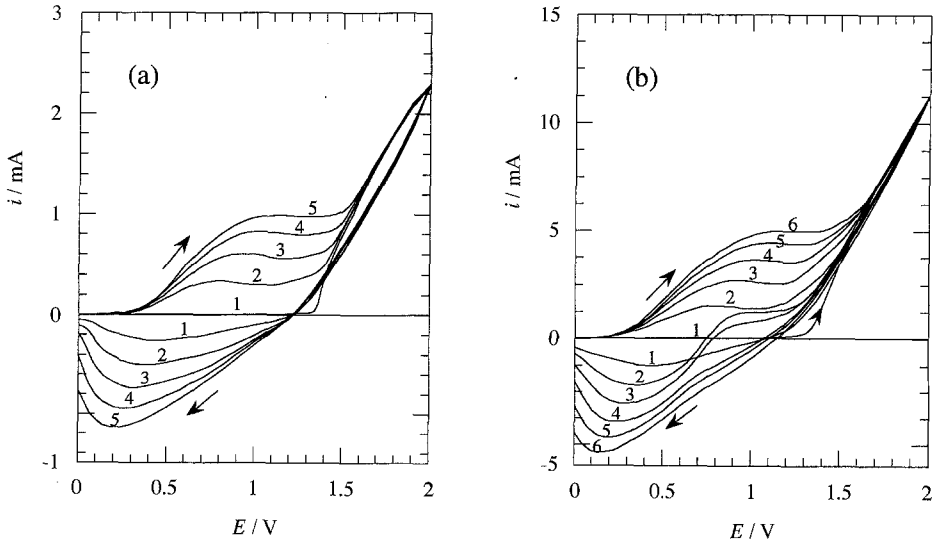

Fig. 6. Cyclic voltammograms for polythiophene formed on 6.2 mm^2 platinum (a) and 0.25 cm^2 stainless steel mesh (b) in acetonitrile solution (monomer concentration: 0.1 M, supporting electrolyte: 0.05 M Me_4NBF_4, scan rate: 100 mV s^{-1}).

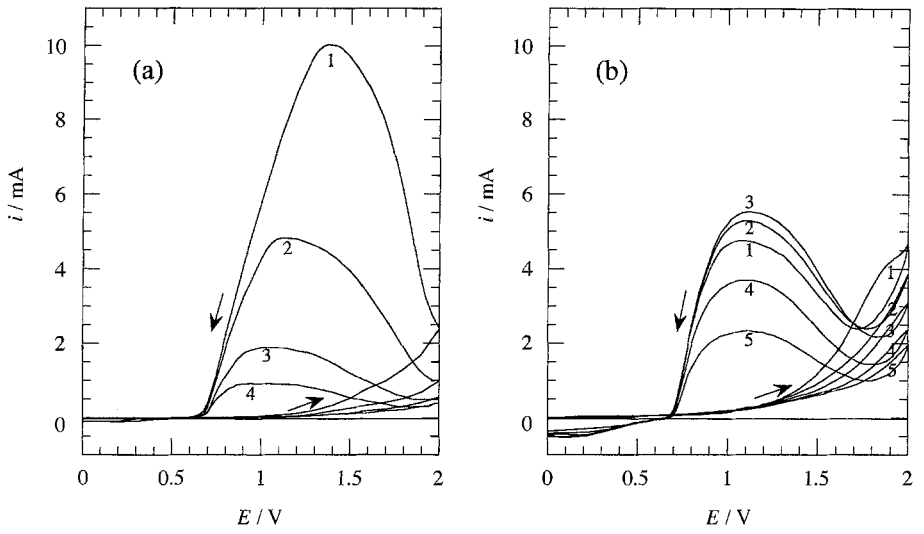

Fig. 8. Cyclic voltammograms show the anodic oxidation of 0.25 cm^2 mesh in acetonitrile solution. (a) Thiophene-free, scan rate: 50 mV s^{-1}; (b) thiophene concentration: 0.01 M, scan rate: 100 mV s^{-1}. 0.05 M Me_4NBF_4 as supporting electrolyte.

resulting from the anodic corrosion. Nevertheless, we cannot exclude the possibility that it is due to some interaction between the substrate and the first layers of PTh. However, deposition on graphite electrodes yielded the same results as on Pt electrodes. In any case, the occurrence of anodic corrosion could be deduced from the shape of CV curves and the position of the switching point.

Evidence for this point of view was obtained by carrying out experiments using Bu_4NBF_4 as a supporting electrolyte: it was noticed that the shoulders on the reverse scans were extraordinarily high, and even after four scans the loops resulting from the shoulders still existed (Fig. 9). This implies a stronger anodic corrosion competing with the PTh deposition.

After investigation of deposition by means of cyclic voltammetry, the samples were observed by SEM. The influence of anodic oxidation of the metal (corresponding to CVs in Fig. 8(a)) and its effect on the deposit (corresponding to CVs in Fig. 9) are illustrated in Fig. 10. As can be seen in Fig. 10(a), after six scans (only the first four of which are shown in Fig. 8(a)), a great number of holes due to corrosion were generated on the wires. When deposition and corrosion occurred at comparable rates, many blister-like defects appeared on the deposition surface (Fig. 10(b)). These were obviously caused by the holes due to corrosion on the fibres. With further polymer deposition, the electrode was increasingly covered and deposition dominated the total electrochemical

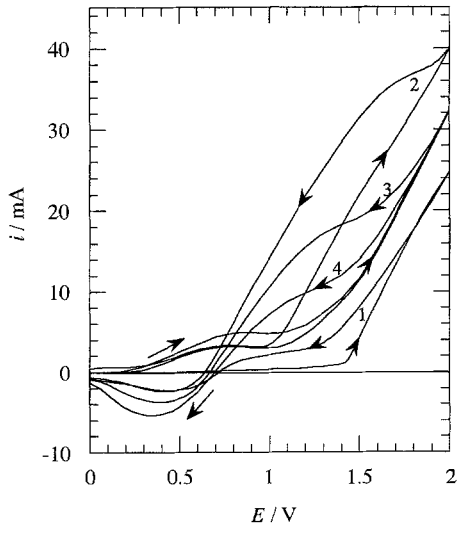

Fig. 9. Cyclic voltammograms for polythiophene formed on 0.25 cm^2 mesh in acetonitrile solution (monomer concentration: 0.1 M, supporting electrolyte: 0.1 M Bu_4NBF_4, scan rate: 100 mV s^{-1}).

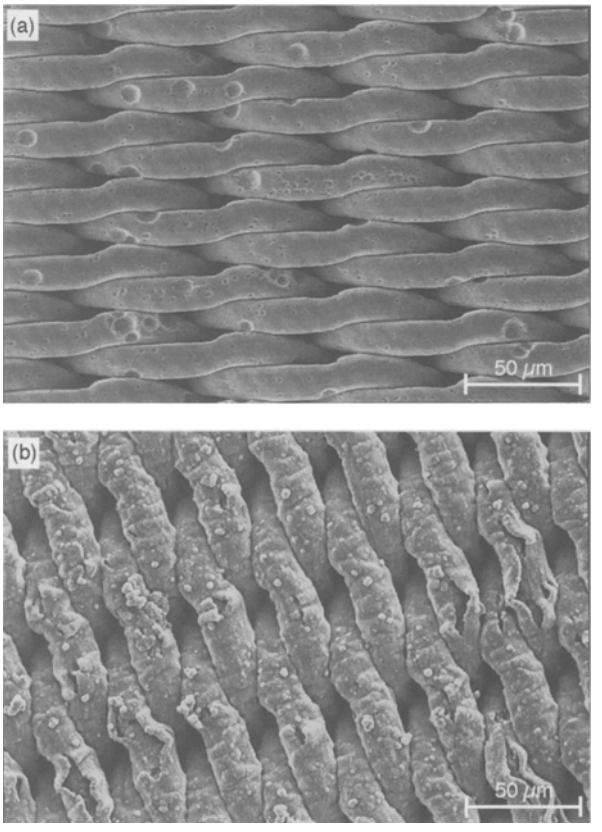

Fig. 10. SEM observation of anodic corrosion and its effect on deposit morphology. (a) Six potential scans from 0–2.0 V at the rate of 50 mV s^{-1} in 0.05 M Me_4NBF_4 thiophene-free solution (CVs of the first four scans are shown in Fig. 8(a)); (b) blister-like defects resulting from initial corrosion of the metal (corresponding CVs are shown in Fig. 9).

process but the trail of the initial corrosion remained in deposits.

Although the electrode oxidation occurred in competition with the polymerization of thiophene, a continuous deposition of high quality PTh was possible, when 0.1 M thiophene containing 0.05 M Me_4NBF_4 or 0.1 M Bu_4NBF_4 solutions were used. Figure 11 reveals the morphology of samples prepared by potential scanning (corresponding CVs are displayed in Fig. 6(b) and Fig. 7) and by constant potential electrolysis. All deposits appeared very compact and adhered well to the fibre, and the defects depicted in Fig. 10(b) were hardly observed. With regard to the surface smoothness, samples prepared by different procedures differed from each other. It has been repeatedly proven that, under the condition of constant potential, samples showed a more uniform surface. In the case of the potential scan mode, deposits prepared at lower scanning rates gave smoother surfaces.

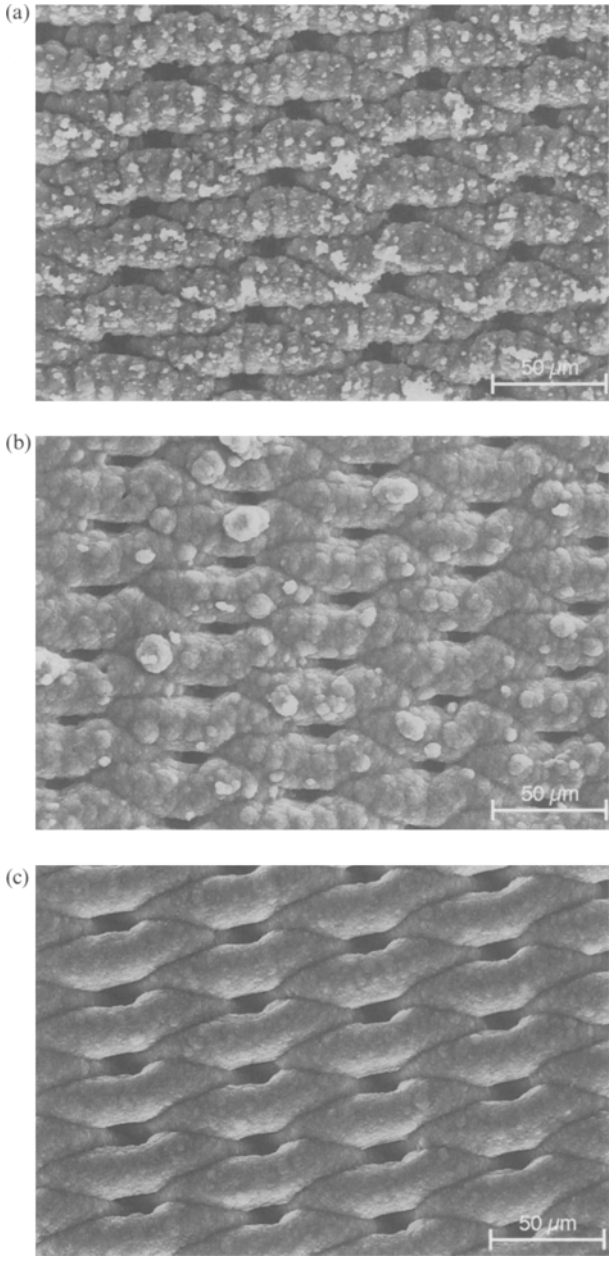

Fig. 11. SEM observation of polythiophene deposited in acetonitrile solutions at different electrochemical conditions (monomer concentration: 0.1 M, supporting electrolyte: 0.05 M Me_4NBF_4). (a) 21 potential scans from 0–2 V at the rate of 100 mV s^{-1} (corresponding CVs of the first six scans are shown in Fig. 6(b)). (b) six potential scans from 0–2 V at the rate of 20 mV s^{-1} (corresponding CVs of the first five scans are shown in Fig. 7). (c) At constant potential of 2.0 V for 7.5 min.

Unlike the successful synthesis of PPy on stainless steel mesh, attempts at depositing PTh on large area stainless steel meshes failed for reasons that are as yet unclear. We were not able to obtain enough deposit without corrosion of the metal under any of the conditions investigated. This is surprising since good polymer layers could be deposited on small areas in the minicell. Possible reasons are:

(i) Usually the diffusion of electroactive reactants to electrodes is not the rate-determining step in the electropolymerization process of thiophene. But due to the large area of the working electrode and the narrow space between the counter and working electrodes, the depletion of the electroactive substance around the electrode could be so important that diffusion could not match the lowest required concentration, which would have made the reaction diffusion-controlled. Consequently, the competitive anodic corrosion dominated, giving rise to a loss of nucleation sites.

(ii) The electrochemical reaction may be influenced by the products from the cathode. In the case of the minicell, the working and counter electrode were placed in two separate compartments, whereas in the preparative cell, they were in a single compartment cell and the distance between the two electrodes was small compared to the electrode size.

Another parameter should nevertheless be investigated. It has been shown that the corrosion of iron in organic media depends on the solvent: strong corrosion is observed in acetonitrile, whereas the rate of corrosion is lower in a less acidic solvent such as methanol, and even no corrosion occurs in THF [37]. Moreover, it has been observed in the study of the electropolymerization of pyrrole on iron electrodes that loops appear on the CVs and that the oxidation leads to mixtures of PPy and iron oxide when the solvent is acetonitrile, whereas normal CVs are observed in THF [38]. Although the conditions for pyrrole and thiophene polymerizations are different, an investigation of the solvent effect could be of interest since an improvement in polymer deposition can be expected from solvents less acidic than acetonitrile.

4. Conclusions

The present study has shown the possibility of applying the electrodeposition technique to the fabrication of dense membranes, which may be used as barriers for gas and liquid separations. The feasibility of this technique depends mainly on two factors: the nature of the monomer to be electropolymerized and the

resistance of the porous substrate to anodic corrosion during the electrochemical process.

Polythiophene showed a very compact and smooth morphology on a small-sized stainless steel electrode, but the high oxidation potential of thiophene led to corrosion of the substrate and, consequently, difficulties were encountered in attempts at deposition on large areas.

Of the two investigated conducting polymers, polypyrrole was the easiest to deposit electrochemically on the substrate. The SEM observation revealed the absence of pin-holes. In the presence of 1 wt % water, PPy doped with hexafluorophosphate (PF_6^-) manifested a more suitable morphology and was selected for further tests of membrane properties. Owing to a large structural variety and doping diversity, membrane properties can be modified to suit diverse applications.

References

[1] J. Heinze, in: E. Stecken (Ed.), 'Topics in Current Chemistry-Electrochemistry IV', Springer-Verlag, Heidelberg (1990) p. 1.
[2] T. Stevens, *Mater. Eng.* **108** (1991) 21.
[3] H. Naarmann, *J. Polymer Sci., Polymer Sympos.* **75** (1993) 53.
[4] J. S. Miller, *Adv. Mater.* **5** (1993) 587.
[5] *Idem, ibid.* **5** (1993) 671.
[6] P. Burgmayer and R. W. Murray, *J. Am. Chem. Soc.* **104** (1982) 6139.
[7] *Idem, J. Phys. Chem.* **88** (1984) 2515.
[8] H. Zhao, W. E. Price and G. G. Wallace, *J. Electroanal. Chem.* **334** (1992) 111.
[9] *Idem, Polymer* **34** (1993) 16.
[10] *Idem, J. Membrane Sci.* **87** (1994) 47.
[11] M. R. Anderson, B. R. Mattes, H. Reiss and R. B. Kaner, *Science* **252** (1991) 1412.
[12] M. R. Anderson, B. R. Mattes, H. Keiss and R. B. Kaner, *Synth. Met.* **41** (1991) 1151.
[13] W. Liang and C. R. Martin, *Chem. Mater.* **3** (1991) 390.
[14] C. R. Martin, W. Liang, V. Menon, R. Parthasarathy and A. Parthasarathy, *Synth. Met.* **55** (1993) 3766.
[15] D. L. Feldheim and C. M. Elliott, *J. Membrane Sci.* **70** (1992) 9.
[16] V. M. Schmidt, D. Tegtmeyer and J. Heitbaum, *Adv. Mater.* **4** (1992) 428.
[17] C. Liu, W.-J. Chen and C. R. Martin, *J. Membrane Sci.* **65** (1992) 113.
[18] J. Mansouri and R. P. Burford, *ibid.* **87** (1994) 23.
[19] I.-H. Loh, R. A. Moody and J. C. Huang, *ibid.* **50** (1990) 31.
[20] P. A. Christensen and A. Hamnett, *J. Electroanal. Chem.* **242** (1988) 47.
[21] J. Bukowska and K. Jackowska, *Electrochim Acta.* **35** (1990) 315.
[22] P. A. Christensen and A. Hamnett, *ibid.* **36** (1991) 1263.
[23] K. M. Cheung, D. Bloor and G. C. Stevens, *Polymer* **29** (1988) 1709.
[24] Z. Deng, W. H. Smyral and H. S. White, *J. Electrochem. Soc.* **136** (1989) 2152.
[25] W. Janssen and F. Beck, *Polymer* **30** (1989) 353.
[26] M. Schirmeisen and F. Beck, *J. Appl. Electrochem.* **19** (1989) 401.
[27] S. Aeiyach, A. Kone, M. Dieng, J.-J. Aaron and P.-C. Lacaze, *J. Chem. Soc., Chem. Commun.* (1991) 822.
[28] G. Troch-Nagels, R. Winand, A. Weymeersch and L. Renard, *J. Appl. Electrochem.* **22** (1992) 756.
[29] F. Beck and R. Michaelis, *J. Coatings Technol.* **64** (1992) 59.
[30] V. Haase and F. Beck, *Electrochim. Acta.* **39** (1994) 1195.
[31] F. Beck and P. Hülser, *J. Electroanal. Chem.* **280** (1990) 159.
[32] M. Zhou, M. Persin, W. Kujawski and J. Sarrazin, *J. Membrane Sci.*, **108** (1995) 89.
[33] A. J. Downard and D. Pletcher, *J. Electroanal. Chem.* **206** (1986) 147.
[34] G. B. Street, T. C. Clarke, M. Krounbi, K. K. Kanazawa, V. Lee, P. Pfluger, J. C. Scott and G. Weiler, *Mos. Cryst. Liq. Cryst.* **83** (1982) 253.
[35] R. J. Waltman, J. Bargon and A. F. Diaz, *J. Phys. Chem.* **87** (1983) 1459.
[36] G. Tourillon and F. Garnier, *ibid.* **88** (1984) 5281.
[37] C. A. Ferreira, S. Aeiyach and P. C. Lacaze, *J. Electroanal. Chem.* **323** (1992) 357.
[38] C. A. Ferreira, S. Aeiyach, M. Delamar and P. C. Lacaze, *ibid.* **284** (1990) 351.